

**Investigation of the generation and propagation of low  
frequency internal waves:  
A case study for the east coast of India**

**A D Rao<sup>a</sup>, S V Babu<sup>a,\*</sup>, K V S R Prasad<sup>b</sup>, T V Ramana Murty<sup>c</sup>  
Y Sadhuram<sup>c</sup> and D K Mahapatra<sup>a</sup>**

<sup>a</sup> Centre for Atmospheric Sciences, IIT Delhi

<sup>b</sup> Department of Meteorology and Oceanography, Andhra University, Visakhapatnam

<sup>c</sup> Regional Centre, National Institute of Oceanography, Visakhapatnam

**ABSTRACT**

SAR (Synthetic Aperture Radar) images in the northwest Bay of Bengal indicate the existence of internal waves and their occurrence and intensity is topography dependent as indicated by in-situ data and satellite information. To complement and comprehend the observations, a three-dimensional Princeton Ocean Model is applied to study the generation and propagation of internal waves. The model domain is configured with a variable curvilinear grid and the input fields comprise bathymetry, initial temperature and salinity, wind stress, air-sea heat flux and tidal information. The numerical investigation indicated a predominant activity of internal waves in the north, and the rationale is three-fold. The first one could be the stable stratification due to fresh water discharge from head-bay major river system, secondly, the significant magnitude/range of the tides and finally, the bathymetry in the coastal waters off Paradip is about 12% shallower compared to that of Visakhapatnam and further south. The cumulative effect of these causes the predominance of internal waves in the north. The core of the energy is essentially in the low-frequency range and the model is able to simulate semi-diurnal and diurnal components reasonably well up to 6 hour frequency (0.162 cph).

*Key words:* Internal waves, stratification, bathymetry, tides, river discharge

---

\* Corresponding author Ph:91-11-26596023 Fax: 91-11-26591386  
Email : sunkara\_babu@yahoo.com

## 1. Introduction

Internal waves occur in the interior stratified region of strong temperature/density discontinuity (thermocline/pycnocline) in the sea. They can be either progressive or standing waves. The ubiquitous internal waves occupy a vast continuum of spatial and temporal scales (Garret and Munk, 1972,1975). The restoring force for these gravity waves is proportional to the product of gravity and the density difference between the adjacent layers. At internal interfaces this difference is much smaller than the density difference between air and water (by several orders of magnitude). As a consequence, internal waves can attain much larger amplitudes than surface waves. It also takes longer for the weak restoring force to return particles to their average position, and therefore internal waves have periods much longer than surface gravity waves. Internal waves have periods between the inertial period ( $2\pi/f$ , where  $f$  is the Coriolis parameter) and the local buoyancy period ( $2\pi/N$ , where  $N$  is the buoyancy frequency). Above the thermocline, particles diverge ahead of the crest and converge behind the crest (or above the trough). This leads to a series of smooth and rough sea surface. Thus, bands of slicks are indicative of convergence and sinking of surface water and if they move shoreward in shallow water they indicate the presence of internal waves (La Fond, 1962). Perhaps the first investigation on internal waves in the Bay of Bengal was carried out in 1953 by repeated bathythermograph observations from a stationary ship (La Fond and Rao, 1954). The presence of internal waves off Hooghly-Brahmaputra delta and in the eastern Andaman Sea during April 1963 from observations was reported earlier (La Fond and La Fond, 1968). Till 1980, most of the studies on internal waves were made utilizing the time series Bathythermograph/CTD measurements from stationary ships. After 80's, the field measurements on internal waves were mostly made from moored buoys with current meters or with the thermister string from stationary ships. A few works on internal waves were made by monitoring slicks on sea surface through satellite sensors (Shen and He, 2005). It has been pointed out (Garret and Munk, 1979) that an abrupt or fairly sharp density interface within the fluid is not all that essential for the existence of waves that owe their restoring force to gravity; any hydrostatically stable density stratification can support "internal waves".

From the available information/literature, if we are to focus the region of dominance of internal waves in the Bay of Bengal and the adjoining seas, we find that the northern Bay and the western side of the Andaman Sea are potential sources of internal waves.

To look at the mechanisms that generate the internal waves in the sea, the tidal forces across the continental slope, variable winds and moving ships/submarines are some means by which the internal waves could be generated. Satellite imageries show internal wave activity along the continental shelf areas. Since the Bay of Bengal receives heavy discharges from the rivers leading to salinity induced stratification with a coastal bias, one may expect the existence and pronounced activity of internal waves in the coastal zone. The temporal and spatial scarcity/limitations of the existing hydrographic measurements preclude one from a precise understanding of internal waves and their variability. It is therefore all the more necessary to have numerical modeling studies to complement and comprehend the available observations.

As a prelude to the current study, it may be mentioned that a few works addressed the internal waves through numerical modeling. The generation and propagation of internal waves was first modeled by Rattray (1960) using a two layer ocean over stepped topography. Internal tides with more realistic stratification and topography conditions were modeled (Baines,1982; Craig ,1988; Sherwin and Taylor ,1990). Holloway and Merrifield, 1999) and shown that the interaction of the barotropic tidal flow with three-dimensional topography is important in determining the vertical component to the flow of water and hence the forcing of the internal tide. A fully three-dimensional, free surface, nonlinear, hydrostatic numerical model is applied for internal tides on the Australian North West Shelf (Holloway,2001). The non-hydrostatic effects, which are important in a wide spectrum of stratified flows and steepening of internal waves are also investigated (Kanaska and Maderich,2003;Wadzuk and Hodges, 2004). These models use realistic stratification, bathymetry and tidal forcing. The uniqueness of the coastal bay is that the density of the surface layers significantly depends upon salinity as well. Hence the study can be similar and applicable in any tropical region, where the runoff and fresh water discharge have a say in the stability of the upper layers.

In the ocean, sound is the only viable means of communication and range finding. The variations in the ocean structure cause fluctuations to develop in the sound field as it travels. At typical sonar operating frequencies, the main cause of these fluctuations are internal waves. These can be strong enough to completely prevent a signal from being detected. Despite numerous applications in several marine fields like Naval warfare, fisheries, oil and energy extraction from sea, water pollution, etc., the internal waves are still least studied feature in the seas around India. Although internal waves leave profound influence in the thermodynamics over the coastal zone, in the

case of high amplitude storm surges, it is believed that they do not significantly contribute to surges. The impact may be seen only in the thermocline region where mixing takes place, having no considerable bearing on the enhancement or reduction of the surge development. In the light of our inadequate understanding of internal waves in the Bay of Bengal, an attempt is made to address the problem from three different facets, viz., i) Satellite imageries ii) In-situ observations and iii) Numerical modeling to arrive at a plausible conclusion for the occurrence, generation and propagation of internal waves in the Bay of Bengal. The first two may be considered as components of data analysis. Taking cue from the recent modeling studies (Holloway,2001), the 3-dimensional Princeton Ocean Model (POM) has been adapted and configured for the east coast of India to study the generation and propagation of internal waves and is discussed in the modeling component.

## **2. Data Analysis**

The location map of the study area, the east coast of India, is shown in Figure 1. The bathymetry of the region, the location of the stations, where the in-situ/SAR observations are available and also the stations, where the model simulations are presented may be seen in the same figure.

### *2.1. Satellite imageries*

The characteristics of internal waves are studied using the imageries taken from Synthetic Aperture Radar (SAR). SAR technology is an active microwave radar imaging technique that has the ability to provide high-resolution images of the earth/ocean and planetary surfaces, independently of solar illumination. Three SAR imageries of the east coast are examined in an attempt to understand the process and phenomenon of internal waves in the coastal waters of India. They are Figure 2(a): Westward propagating Coastal Oceanic IW packets (Rectangular Boxes) on 15<sup>th</sup> Sep 1995 of European Remote sensing Satellites (ERS)/SAR for the latitudinal extent of 18<sup>o</sup>23' N to 19<sup>o</sup> 08' N, Figure 2 (b): ERS-2 satellite imagery for 13 April 1996 for nearly the same latitudinal extent and Figure 2(c): Envisat image of 4 October 2003 from 19<sup>o</sup> 17' N to 19<sup>o</sup> 43' N.

The SAR profiles ascertain groups of internal wave packets, characterized by several dominant features. Initially single wave of depressions propagating towards the coast and immediately when crossing the continental shelf edge those evaluated as rank ordered internal wave packets. The individual oscillations are non-sinusoidal, with predominantly downward displacements, the amplitudes are rank ordered with the

largest at the front of the packet and the smallest at its rear; wavelengths and crest lengths are also rank ordered, with the longest waves again at the front of the group and the number of individual oscillations within the packet increases as its moves towards the coast. From the profile transect analysis; one can infer that the wave lengths of internal waves decrease from right to left. To understand the influence of the coastal zone bathymetry on the surface signature of internal waves, we need to take the support of the Figure 3 (which will be discussed in the numerical modeling component) that depicts the near-shore depth along the coastline. Now when we analyze the features in Figure 2 (a), it may be noticed that the average depth of the coastal waters in the southern zone is about 130 meters, fairly deep compared to the northern zone, where the depth is less than 60 meters. The bathymetry influence is clearly seen and it may be noticed that the internal wave activity is more prevalent in the northern zone. Even in Figure 2 (b) the surface signatures due to internal waves influenced by bathymetry is also seen with the manifestation being more conspicuous in the northern zone. The internal waves are believed to be generated by the strong flow over the shelf edge. A feature of interacting/converging internal wave packets may be due to the tidal currents, variable with topography. Figure 2(c) shows substantial shoreward propagating of internal waves over the shelf waters of north Bay of Bengal. It may be noticed that the average depth of the near coastal waters in the southern zone is shallow and is less than 60 meters, while in the north it is above 150 meters (figure3). Hence the more prominent feature of internal wave imagery is in the southern region, in concurrence with the associated bathymetry. Thus it may be noted that the first two SAR imageries dwell in the transition zone of the bathymetry, getting shallower towards north while the third is in a region which is relatively deeper towards north. Further the Envisat ASAR imagery on 26 September 2006 (not shown) for the latitudinal belt of  $17^{\circ} 20' N$  to  $17^{\circ} 34' N$  show no clear signature of internal waves. There are two rivers, Krishna and Godavari in the model domain near  $16^{\circ} N$  on the east coast. Sometimes a very faint local signatures or discharge/current interactions noticed in the region.

Thus, the available SAR pictures provide a message that the imageries, located north of  $18^{\circ} 20' N$  depict clear signatures of internal waves and their occurrence and intensity seem to be dependent on the bathymetry of the region. It may be noticed that the prevalence and intensity reflects the topographic gradient. As mentioned earlier, the rest of the available SAR imageries do not show the dominance of internal waves. This leaves an impression that the southern coastal waters of the bay are not quite favorable

for the generation of internal waves *to the extent of being detected by SAR imageries*. This is because although the non linear internal waves are ubiquitous underneath the mixed layer, the surface expression is a function of their amplitudes that modulates the zones of convergence and divergent patterns at the surface.

## 2.2. *In-situ Observations*

The Regional Centre of NIO, Visakhapatnam collected time series data using CTD/Thermister chain/current meter, from 15<sup>th</sup> February to 15<sup>th</sup> March 2004 at Vodalarevu (location: Lat 16°15' N and Lon 82° 11' E) and during 23-25 February 2007 at Bhimili (location: Lat 17°36' N and Lon 83° 42' E). The time interval of the data collection is hourly for CTD and two minutes for thermister chain and current meter, sufficient for the analysis of low frequency internal waves. Both observations are nearly of the same period of the year (although the years are different). Unfortunately, the in-situ observations and the satellite imageries are not available for the same region/period. The data has been analyzed for the energy spectrum in frequency bands of internal waves and subjected to Fast Fourier Transform (FFT) to examine the spectral characteristics of the temperature oscillations in the study area off Vodalarevu and Bhimili (Mahadevan et.al, 1987). An overview of the spectrum analysis is discussed below.

Spectral estimates (of temperature oscillations) have been obtained by using the Fast Fourier Transform algorithm of Cooley and Tukey (1965) using Hanning window function. The power spectra of temperature fluctuations were computed to study the internal waves with one ensemble data set and are presented in Figure 4. In general, the energy associated with the internal waves is essentially in the low frequency range compared to that of high frequency and the maximum energy seems to be in the thermocline region. In-situ time series data is available at 5m, 50m and 100m depth. The energy spectrum using the time series temperature data is therefore computed for low frequency (less than 0.5cph) at these depths. Figure 4 shows the spectral estimate at these depths at both locations. One may find considerable differences in the energy spectrum. It may be noticed that at the southern location, Vodalarevu, (right panel), the crux of the energy in the low frequency spectrum is focused at 0.08 cph (12.5 hour semi-diurnal), where as at Bhimili (left panel), the energy is considerably low and also got distributed over different frequencies, indicating a fall in energy in the low frequency spectrum; might be owing to mixing, bottom friction etc. If we analyze the energy spectrum in the light of the bathymetry around for both the locations, the local depth is comparable but the off-shore topography shows considerable differences. At

Vodalarevu, it is relatively deeper and regular, while at Bhimili, it is shallower. As the tide is a body force, altered by the shape of the basin and sea floor configuration, the topographic gradients result in inducing dynamical interactions with the slopes. The role of internal tides on the continental shelf has long been recognized (Rippeth and Inall, 2001) to this effect. The tide interaction with the shallower bathymetry at Bhimili may therefore be relatively enhanced and liable for more conversion of the initial energy associated with the tide in the lower spectrum to higher frequencies as the resulting internal wave of tidal period breaks up into waves of shorter period, while propagating onshore.

A brief note of the inferences from the previous works that endorse the model simulations are mentioned here. Internal waves arise within a wide range of frequencies – from short period waves with periods  $T \sim 10 \text{ S}^{-1}$  to internal waves with periods of days. Those waves with astronomical tidal periods – the so called baroclinic tides – occupy a central place because they are more intensive and more pronounced in the ocean than most others. Calculations of power spectra for various sites of the world ocean have shown that at practically all locations a peak can be found in the spectral density which is in the vicinity of the tidal frequency. Gregg and Briscoe (1979) estimated that one-third of all vertical displacements related to internal waves can be assigned to baroclinic tides. An analysis by Muller and Briscoe (2000) has confirmed the observation of spectral peaks at the inertial and semidiurnal tidal frequencies. Being more energetic, the baroclinic tides spread out their energy through the spectrum from large to small scales due to different interactions and thus tend to develop universal spectral distribution, as was first recognized by Garret and Munk ( 1972), specified more recently by Hibiya et al (1998).

### **3. Numerical modeling**

#### *3.1. The Model and Methodology*

To study the response of the coastal ocean due to the generation and propagation of internal waves, a three-dimensional Princeton Ocean Model, as described in detail (Blumberg and Mellor, 1987; Mellor, 1992) has been configured for the east coast of India. It is a free surface ocean model with a turbulence closure scheme (Mellor and Yamada, 1982). The momentum equations are nonlinear and incorporate  $\beta$ -plane approximation. The model uses an orthogonal curvilinear grid and a terrain following sigma coordinates in the vertical. The analysis region and the associated bathymetry are as discussed in model bathymetry below. The off-shore width

of the model domain is 400-500 km and the coastal stretch is about 1400 km, extending from 12° N to about 22° N. There are 200 x 100 grid points in the horizontal plane and 26 sigma levels in the vertical. The resolution in the x - direction varies from 2.5 - 5.0 km, finer near the coast. In the y-direction, the resolution varies from 13.6-18.7 km. The main advantage of the non-uniform grid is the computational resources are more efficiently utilized. The two-dimensional external mode uses a short time-step of 10 sec while a three-dimensional internal mode uses a long time-step of 300 sec.

The surface forcing includes the wind stress and heat flux that comprises of incoming short wave radiation, outgoing long wave radiation, sensible and latent heat. Apart from the surface forcing, tidal forcing is also incorporated along the eastern open boundary. The numerical experiments are carried out to amalgamate the results with the existing in-situ and satellite (SAR) information to the extent possible. We have SAR imageries in September, October and April and in situ observations mainly in February. October is a transition month and April is an adjoining month to in-situ data (February). Hence, in the light of the available data sets, the numerical experiments are carried out for September and February. Numerical experiments involve the use of both diagnostic and prognostic modes. In the prognostic mode, the momentum equations as well as equations governing the temperature and salinity distributions are integrated as an initial value problem. These predictive experiments do not always reach a steady state because the oceanic response time for the density field can be considerable. To produce circulation fields, the model has been spun up from rest for 15 days with the corresponding monthly forcing fields, temperature and salinity, held fixed in time. For POM in the diagnostic mode, 5 to 7 days spin-up time was shown to be sufficient for circulation to approach equilibrium with the forcing fields (Ezer and Mellor, 1994). The experiments in the diagnostic mode attain quasi steady-state conditions. The diagnostic approach not only provides a powerful tool for deducing circulation but also permits a consistent way of initializing a prognostic mode.

***The basic inputs to the model are as follows:***

**A) Bathymetry:** The bathymetry is derived from the modified ETOPO2 (Sindhu et al, 2007), which is shown in the Figure 1(a). The modified data set is more accurate in depths less than 200 meters and therefore improves the performance of the numerical models in the coastal zone. A bilinear interpolation has been used to obtain depths at computational grid points to smoothen the topographic gradients that could otherwise cause spurious along-slope currents in a sigma coordinate model (Haney, 1991). The

bottom topography varies sharply in coastal zone, north of 18°30'N showing along-shore gradient which is sensitive to the generation and propagation of internal waves. This transition zone is zoomed and is shown in Figure 1(b). Further, a closer look at the near-shore bathymetry along the coastline is shown in Figure 3.

**B) Temperature and salinity:** The model uses initial data fields of temperature and salinity as initial density field derived from the World Ocean Atlas 2001 (WOA01), of National Oceanographic Data Center, (<http://ingrid.ldeo.columbia.edu/SOURCES/.NOAA/.NODC/.WOA01/.Grid-1x1/.Monthly/.an/>). It may be noted that salinity is measured using the Practical Salinity Scale. The objectively analyzed climatological monthly mean fields, available at 24 standard depths upto 1500 meters are used.

**C) Winds:** The model is forced with mean monthly climatological wind stress, inferred from COADS winds (da Silva et.al, 1994) available at 1° resolution.

**D) Surface heat fluxes:** The air-sea heat flux climatology has been obtained from the Southampton Oceanography Centre (SOC), available from (<http://ingrid.ldeo.columbia.edu/SOURCES/.SOC/.GASC97/>). In generating the climatology, estimates of the fluxes have been obtained from the in-situ reports within the COADS 1a (Comprehensive Ocean Atmosphere Dataset 1a), a global dataset comprising about 30 million surface observations from ships and buoys collected over the period 1980-93. The reported meteorological variables, used to calculate the fluxes have been corrected for various observational biases using additional information about measurement procedures which has been blended in from the WMO47 list of ships.

**E) Tides:** The internal waves are commonly observed on many continental shelves around the world. In-situ measurements and SAR imageries show the packets of internal waves near the shelf break during stratified conditions. The temporal and spatial separations of these packets suggest that they evolve from internal tides generated by the semidiurnal tidal currents advecting the stratified fluid over the steep topography. The semidiurnal tidal flow is dominated by the principal lunar constituent M2 (12.42 hour period) in the Bay of Bengal although other components also contribute in different time scales. Hence, we need to obtain tidal information that should be incorporated in the model for the study of generation and propagation of internal waves by specifying the tidal forcing on the eastern open-boundary. Tides are a significant contributor to the sea

surface height and they have more variation than most other time-varying ocean signals. The response of a thermal/saline stratified ocean to tidal and wind forcing is studied using the numerical model.

The tidal elevation is derived from the Global Ocean Tidal Model from TOPEX/POSEIDON Altimetry (software for the computation of tides from the **Finite Element Solution, FES2004**, from NASA, Maryland). The ocean tide model incorporates the astronomical components and also utilizes processed T/P and ERS data assimilation in the hydrodynamical solution. The data includes the M2, S2, N2, K2, K1, O1, P1, Q1 and S1 tides. The model can calculate tide level for any arbitrary date, time and location. After obtaining the tide information all along the open-boundary, the associated tidal current is incorporated as normal velocity.

The boundary conditions in the vertical are no-slip condition at the bottom and no through flow at the surface for the continuity equation. For the momentum equations, the boundary conditions are suitably specified using the surface and bottom turbulence momentum fluxes. The boundary conditions for velocities include radiation conditions at the lateral open boundaries. The details of the methodology are given by Babu et al (2008).

### *3.2 Results and discussion*

At the outset it may be pertinent to mention the limitations of the model. The first one is the constraint imposed by the model being hydrostatic. The second one is because of the smoothed climatological energy inputs at the sea surface, where there are no short-term fluctuations and meso-scale variations in winds. As high frequency fluctuations are associated more with diurnal variations (Mc Phaden et.al, 1992), realistic surface energy processes on the corresponding scales are of prime importance in resolving them. However, the core of the energy of the internal waves is essentially in the low frequency range and the numerical model is able to simulate the same (semi-diurnal, diurnal and inertial) and the associated oscillations reasonably well in different experiments. Further, the satellite Data or in-situ observations over Bay of Bengal are few and far between and are not adequate to offer a definite conclusion.

Notwithstanding the constraints, numerical modeling experiments are carried out to investigate the dynamics of the internal waves of the Bay of Bengal. In the first experiment, model simulations are carried out for September. Heat fluxes of September and October are utilized in integration, which is consummated by gradually imposing the fluxes from September through October as the model integration progresses with time.

As our prime concern is the shelf region, where the progression of the internal waves is seen to be normal to the coast (as is evident from the satellite imageries), we impose the tidal forcing only along the eastern open boundary. The tide data for September (arbitrarily for, 2005) is obtained by using FES2004. Two extreme locations on the eastern open boundary are chosen, one at north ( $T_1$ ) and the other at south ( $T_2$ ) as shown in Figure 1(a). The tidal elevations at  $T_1$  and  $T_2$  are derived and shown as dashed and solid lines respectively in Figure 5. The maximum amplitude of the tide at  $T_2$  is about 25 cm where as it is about 100 cm at  $T_1$  during the first fortnight of the month. Although the tidal range at these locations is very different, they are in phase. Therefore, the tide amplitude along the open-boundary at each grid point is conveniently obtained by interpolation. Having known the tidal amplitudes, the tidal forcing is incorporated normal to the eastern boundary as the ensuing geostrophic current, which is in accordance with the local tidal amplitude. With the combined climatological forcings of wind stress and flux of September-October together with tide, the model is integrated for 32 tidal cycles (16 days) and subsequently the simulations are analyzed. Figure 6 depicts the surface current, which is close to the typical monsoon circulation, characterized by counter-rotating eddies (Hareesh kumar et.al, 2001) in the Bay of Bengal. The northern (upper) and southern (lower) regions of the model domain are shown to the right with enhanced resolution. The circulation is driven by an intricate combination of wind, differential distribution of freshwater in the surface layers and tidal effects. The surface signature of divergence/convergence bands may be attributed to the propagation of internal wave crests/troughs below. However, this is discernable more in the north, particularly offshore. The current at the coastal boundary is probably hampering the signatures being perceptible there.

To understand how the internal wave activity varies along the coast, vertical transects of temperature off three selected stations, Chennai (south), Visakhapatnam (middle) and Paradip (north) are chosen. The transects extend up to approximately 250 km from the coast. Figure 7(a, b, c) shows the model simulated vertical temperature ( $^{\circ}\text{C}$ ) respectively off these stations. It may be noticed that the temperature oscillations and hence the internal wave activity is being enhanced from south (Chennai) to north (Paradip) beneath the surface layers. At Chennai, a moderate tide influence is seen only below 100m depth. At Visakhapatnam, the temperature oscillations are enhanced compared to that of Chennai. At Paradip, the oscillations further increased by more than one meter amplitude (compared to that at Visakhapatnam) in the 100m depth zone. One of the contributing factors for augmentation in the activity of internal waves is the stability

of the surface waters, which is significantly high in the northern region. This is evident from the fact that the vertical salinity gradient is about 0.6/m in the coastal zone off Paradip, whilst it is about 0.2/m at Chennai in the surface layers up to top 10m. A horizontal surface salinity variation of about 4 is also noticed between these two stations.

The model simulations are carried out in the next experiment for February. The time variant surface forcing consists of heat fluxes of February and March and February wind stress. The tidal elevations at  $T_1$  and  $T_2$  for February (arbitrarily for 2007) are not shown here but are similar to the oscillations of September 2005. The maximum amplitude of the tide at  $T_1$  is about 30 cm and at  $T_2$  it is about 125 cm. With the forcings of wind stress, flux and tide, the model is integrated for 32 tidal cycles as before. To complement/ascertain the inference from the simulations of the previous numerical experiments, the model simulations at the same stations are considered. However, instead of vertical cross-sections, time-sections of temperature are depicted in Figure 8(a, b, c), where the local depth is about 200m. The tidal forcing that is applied along the eastern open boundary takes about 4-5 days (lag) to reach the near coastal zone and consequently, there are no associated fluctuations in temperature until 4 days. Hence, the time sections are shown beginning with four days of model integration. It may be noticed that the temperature oscillations associated with the internal wave activity is pronounced from south (Chennai) to north (Paradip) and their amplitude is in accordance with the tidal forcing attached with the lag of 4-5 days. The tidal elevations gradually increase up to day 5 and start to wane subsequently. As the lag is about 4-5 days, the waning in the temperature oscillations in Figure 8(a, b, c) begins only after about 10 days. The amplitude in temperature oscillations at the coastal waters is also consistent with the tidal oscillations at their corresponding latitude. This may be ascertained by the small amplitude in temperature oscillations at Chennai (Figure 8a) corresponding to the small amplitude in tidal oscillations at the southern location, similar as in the case of September 2005. This gives an indication that the tide leaves a definite bearing on the internal waves, apart from the bathymetry. Further, a model test runs has been carried out with uniform depth (of 500 meters) which could not generate internal waves much, indicating the role and importance of shoaling bottom of the continental shelf. Also another experiment with weak stratification was carried out which reveal that the energy/amplitude of the internal waves is much less.

To examine further its dynamic interaction with the bottom topography from the energy considerations, two locations are chosen in order to facilitate a qualitative comparison with the available in-situ data analysis. Bhimili, with shallow off-shore bathymetry, 'the *shallow station*' and Vodalarevu, a relatively corresponding '*deep station*' are shown in Figure 4. The location of the stations along the coast is shown in Figure 1. At these two locations, time series model simulated temperature is extracted at a time interval of 2.5 minutes at 90m (the average depth of the seasonal thermocline over the model domain is about 100m in February) as the model integration goes over 16 days. The energy spectrum using this data is computed as in the case of *in-situ* observations for low frequency in two parts, i) 0 to 0.12 cph. i.e., up to ~ 8 hour frequency and ii) 0.25 cph to 0.12 cph i.e., 4 to 8 hrs frequency interval. Figure 9(a, b) shows the spectral estimate for the lower frequency at the *shallow* and *deep stations* respectively. The core of the energy in this low frequency spectrum is focused at 0.08 cph (12.5 hour semi-diurnal frequency), although spectral peaks corresponding to inertial and diurnal frequency are also evident. However, one may find considerable differences in the spectral estimates, which is much higher at the *deep station*. In this context it may be pertinent to note that the spectral estimates of Vodalarevu (Figure 4, right panel) and the model simulations are comparable, besides the fact that in both cases, the crux of the energy is focused at 0.08 cph, the semidiurnal frequency. Figure 9(c,d) shows the spectral estimate for the higher frequency at *shallow* and *deep stations* respectively. It may be noticed that the maximum energy is focused at 0.162 cph, i.e., ~ 6 hour freq. Contrary to the energy levels in the lower frequency spectrum, the energy associated with the higher frequency spectrum is much less in the *deep station*. If we analyze the energy spectrum again in the light of the bathymetry for both the *stations*, we may infer that the tide interaction with the shallow bathymetry is relatively enhanced and liable for more conversion of the initial energy, associated with the tide in the lower frequencies to higher frequencies as the internal wave of tidal period breaks up into waves of shorter period, while propagating onshore.

#### **4. Conclusions**

In the Bay of Bengal, the nearshore bathymetry of the east coast of India tends to be shallow north of 18°30'N. The alongshore topographic gradient that dwells in the coastal region in the north is also favorable to the generation of internal waves. Further, the northern Bay of Bengal shows a perennial gradient in salinity, both in the horizontal

and in the vertical, which enhances the bathymetric effect. The larger tidal range in the north also contributes for the more prevalence of internal waves in the northwest Bay of Bengal. The simulations are reasonably sound and definitely contribute to the understanding of the physics and phenomenon of internal waves qualitatively well as the energies associated with low frequency spectrum compares quite well with the observations in most cases. The model could resolve the frequency of oscillations on the higher side upto 0.162 cph which corresponds to 6 hours only. However, the core of the energy of the internal waves is essentially in the low frequency range and the numerical model is able to simulate the same (semi-diurnal, diurnal and inertial) and the associated oscillations reasonably well in different experiments. To mention the limitations of the study, satellite Data or in-situ observations over Bay of Bengal are few and far between and are not adequate to offer a definite conclusion. As part of conclusions, we put together the available information and outcome of the current study in an attempt to assimilate and understand the Bay of Bengal dynamics with regard to internal waves. It is true that internal waves are ubiquitous phenomenon in the ocean. However, conspicuous predominance is not everywhere. The model simulations suggest that the variation of the tidal range as well as stratification have a definite bearing on the generation and propagation of internal waves. Thus the study brought out certain important and useful results that a) satellite observations b) In-situ observations and c) model simulations all corroborate among themselves.

## **5. Acknowledgements**

We sincerely thank the Naval Research Board (India) for providing the financial support during the course of the study. Our sincere thanks are also due to the European Space Agency for providing the required satellite imageries. Thanks are also due to Mr. M.Rajasekhar, JRF, Department of Meteorology and Oceanography, AU, Visakhapatnam for his assistance in the analysis of SAR imageries. We sincerely thank the reviewers for their meticulous care and attention in improving the quality of the article.

## **References**

- Babu, S.V., Rao, A.D., Mahapatra, D.K., 2008. Pre-monsoon variability of ocean processes along the east coast of India, *Journal of Coastal Research* 24 , 628-639
- Baines, P.G., 1982. On internal tide generation models, *Deep Sea Research, Part A*, 29 307-338.

- Blumberg, A.F., Mellor, G.L., 1987. A description of a three dimensional coastal ocean circulation model in Three-Dimensional Coastal Ocean Models, AGU, Washington, D. C.,
- Cooley, J.M., Tukey, J.W., 1965. An algorithm for the machine calculation of complex fourier series, *Mathematics of Computation* 19, 297 - 301.
- Craig, P.D., 1988. A numerical model study of internal tides on the Australian North West Shelf, *Journal of Marine Research* 46, 59-76.
- da Silva, A., Young, C, Levitus, S., 1994. Atlas of Surface Marine Data 1994, Volumes 1–5. Washington, DC: U.S. Department of Commerce NOAA atlas NESDIS 6–10
- Ezer, T. and G. L. Mellor, 1994, Diagnostic and prognostic calculations of the North Atlantic circulation and sea level using a sigma coordinate ocean model. *Journal of Geophysical Research.*, 99(C7), 14,159-14,171.
- Garret, C.J.R., Munk, W.H., 1972. Space time scales of internal waves. *Geophysical Fluid Dynamics* 3, 225-264.
- Garret, C.J.R., Munk, W.H., 1975. Space time scales of internal waves. A progress report. *Journal of Geophysical Research* 80, 291-297.
- Garret, C.J.R., Munk, W.H., 1979. Internal waves in the ocean. *Annual Review of Fluid Mechanics*. 11, 339-369.
- Gregg, M.C., Briscoe, M.G., 1979. Internal waves, fine structure, microstructure and mixing in the ocean. *Reviews of Geophysics and Space Physics* 17, 1524-1547
- Haney, R.L., 1991. On the pressure gradient force over steep topography in sigma coordinate ocean models, *Journal of Physical Oceanography* 21, 610 -619.
- Hareesh Kumar, P.V., Prasada Rao, C.V.K., Swain, J., Madhusoodanan, P., 2001. Intra-seasonal oscillations in the central Bay of Bengal during summer monsoon 1999, *Current Science* 80, 786-790.

- Hibiya, T., Niwa, Y., Fujiwara, K., 1998. Numerical experiments of nonlinear energy transfer within the oceanic internal wave spectrum. *Journal of Geophysical Research* 103, 18715-18722.
- Holloway, P.E., Merrifield, M., 1999. Internal tide generation by seamounts ridges and islands, *Journal of Geophysical Research* 104, 25,937- 25, 951.
- Holloway, P.E., 2001. A regional model of the semidiurnal internal tide on the Australian North West Shelf, *Journal of Geophysical Research* 106, 19,625 – 19,638.
- Kanarska, Y., Maderich, V., 2003. A non-hydrostatic numerical model for calculating free-surface stratified flows, *Ocean Dynamics* 53 , 176-185.
- LaFond, K.G., Rao, C.P., 1954. Vertical oscillations of tidal periods in the temperature structure of the sea, *Andhra University Memoirs* 1, 109-116.
- LaFond, E.C., 1962. Internal waves. In: M.N.Hill(ed), *The Sea* , Vol. 1, John Wiley&Sons New york, pp.731-751.
- LaFond, E.C., LaFond, K.G., 1968. Studies of oceanic circulation in the Bay of Bengal, *Bulletin of National Institute of Science. India*, 38, 164-183.
- Mahadevan, R., Swaminathan, T., Issac Martin, M., 1987. Ocean surface wave analysis, TR. No. 27 , Ocean Engineering Center I.I.T. Madras pp. 115.
- McPhaden, M.J., Peters, H., 1992. Diurnal cycle of internal wave variability in the equatorial Pacific Ocean: Results from moored observations. *Journal of Physical Oceanography* 22, 1317-1329.
- Mellor, G.L., Yamada, T., 1982. Development of a turbulence closure model for geophysical fluid problems, *Reviews of Geophysics* 20, 851– 875.
- Mellor, G.L., 1992. User's guide for a three-dimensional, primitive equation, numerical ocean model, report, 35 pp., Program in Atmospheric and Oceanic Sciences, Princeton Univ., Princeton, N. J.
- Muller, P., Briscoe, M.G., 2000. Dynamical mixing and internal waves. *Oceanography* 13 , 98-103.

- Rattray, M., 1960. On the coastal generation of internal tides, *Tellus* 22 , 54-62.
- Rippeth, T.P., Inall, M.E., 2002. Observations of the internal tide and associated mixing across the Malin Shelf, *Journal Geophysical Research* 107, 3028, DOI: 10.1029/2000JC000761
- Shen, H., He, Yi-Jun., 2005. Study Internal Waves in North West of South China Sea by Satellite Images, proceedings of Geoscience and Remote Sensing Symposium, Volume: 4, Institute of Electrical and Electronics Engineers, pp 2539-2542.
- Sindhu, I., Suresh, I., Unnikrishnan, A.S., Bhatkar, N.V., Neetu, S., Michael, G.S., 2007. Improved bathymetric data sets for the shallow water regions in the Indian Ocean, *Journal of Earth System Science* 116, 261-274.
- Sherwin, T.J., Taylor, N.K., 1990. Numerical investigations of linear internal tide generation in the Rockall Trough, *Deep Sea Research* 10 , 1595 -1618.
- Wadzuk, B.M., Hodges, B.R., 2004. Hydrostatic and Non-hydrostatic Internal Wave Models, Final Report to the Office of Naval Research under Contract No. N00014-01-1-0574, CRWR Online Report 04-09  
<http://www.crwr.utexas.edu/online.html>).

### **Legends to Figures**

- Figure 1: Location map of the study area: (a) Model analysis area and bathymetry (m) and (b) Bathymetry of the model domain in the transition zone
- Figure 2: (a) ERS SAR imagery, showing the westward propagating coastal oceanic internal waves on 15 September 1995 for the latitudinal extent of 18<sup>o</sup>23' N to 19<sup>o</sup> 8' N, (b) ERS-2 SAR imagery, showing shoreward propagating internal waves on 13 April 1996 from 18<sup>o</sup>20' N to 19<sup>o</sup>10' N and (c) Envisat Image on 4 October 2003 for the latitudinal belt of 19<sup>o</sup>17' N to 19<sup>o</sup>43' N.
- Figure 3: Near-shore bathymetry (m) along the coastline.
- Figure 4: Energy spectra of temperature oscillations for frequencies <0.5cph at depths 5m, 50m and 100m off Bhimili and Vodalarevu
- Figure 5: Tidal elevations at the northern (dashed) and southern (solid) open boundaries in September 2005.

Figure 6: Model simulated surface horizontal current for September.

Figure 7: Model simulated vertical temperature ( $^{\circ}\text{C}$ ) off (a) Chennai (b) Visakhapatnam and (c) Paradip in September.

Figure 8: Model simulated temperature ( $^{\circ}\text{C}$ ) time-sections off (a) Chennai (b) Visakhapatnam and (c) Paradip in February.

Figure 9: Energy spectra of temperature oscillations at depth 90 meters off shallow region (a, c) and deeper region (b, d) in February.

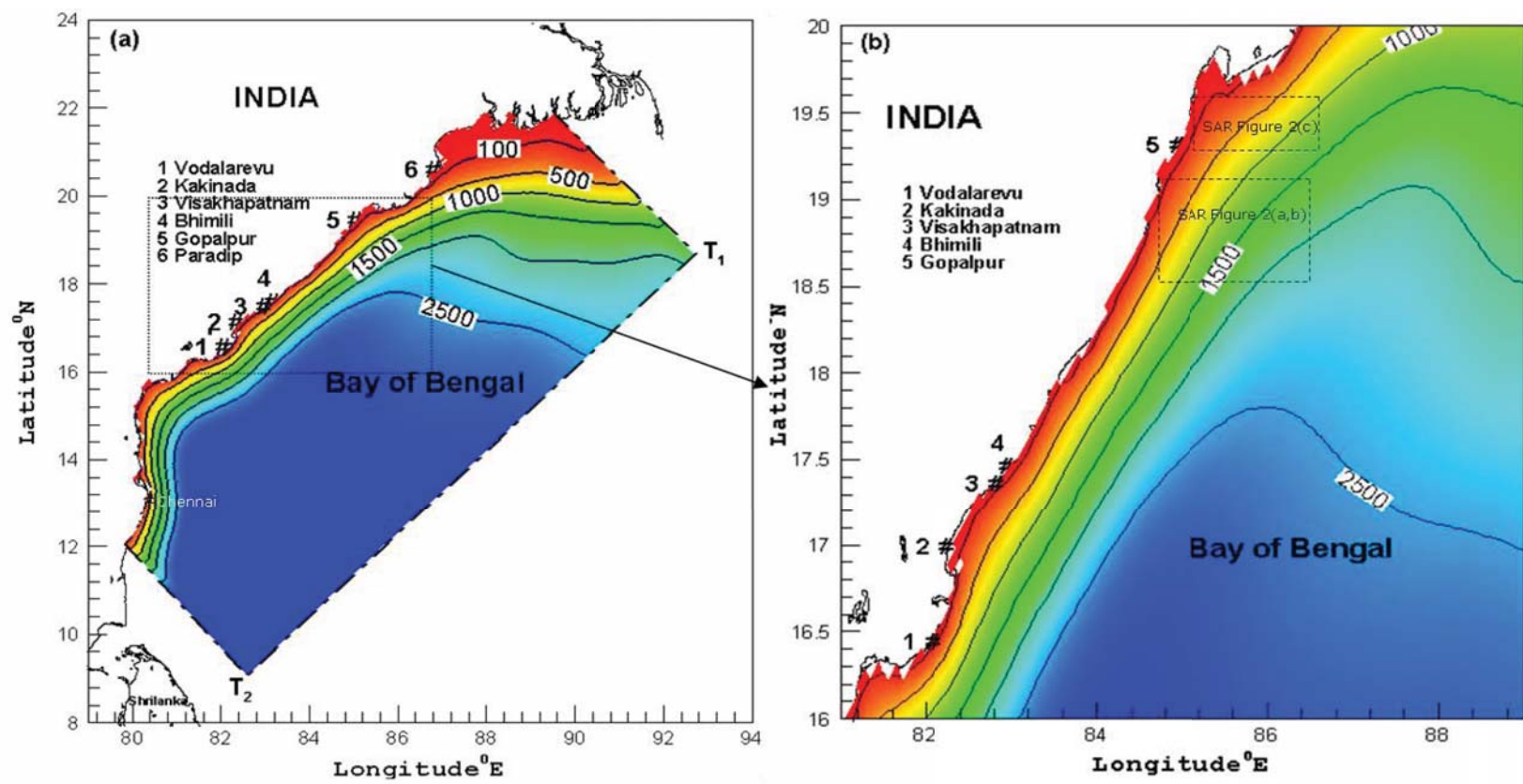


Figure 1

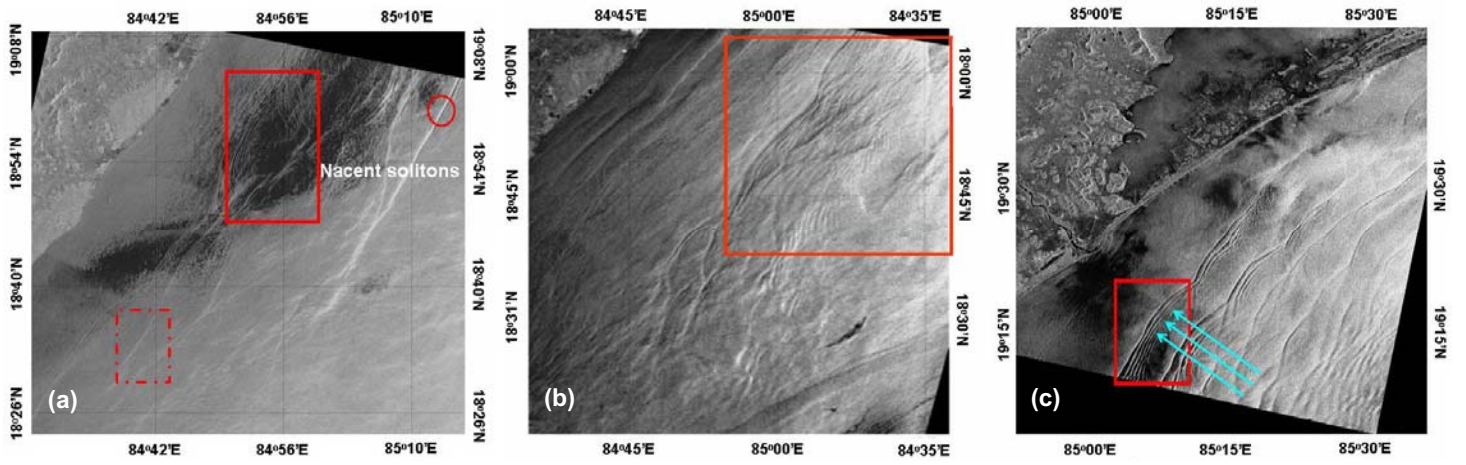
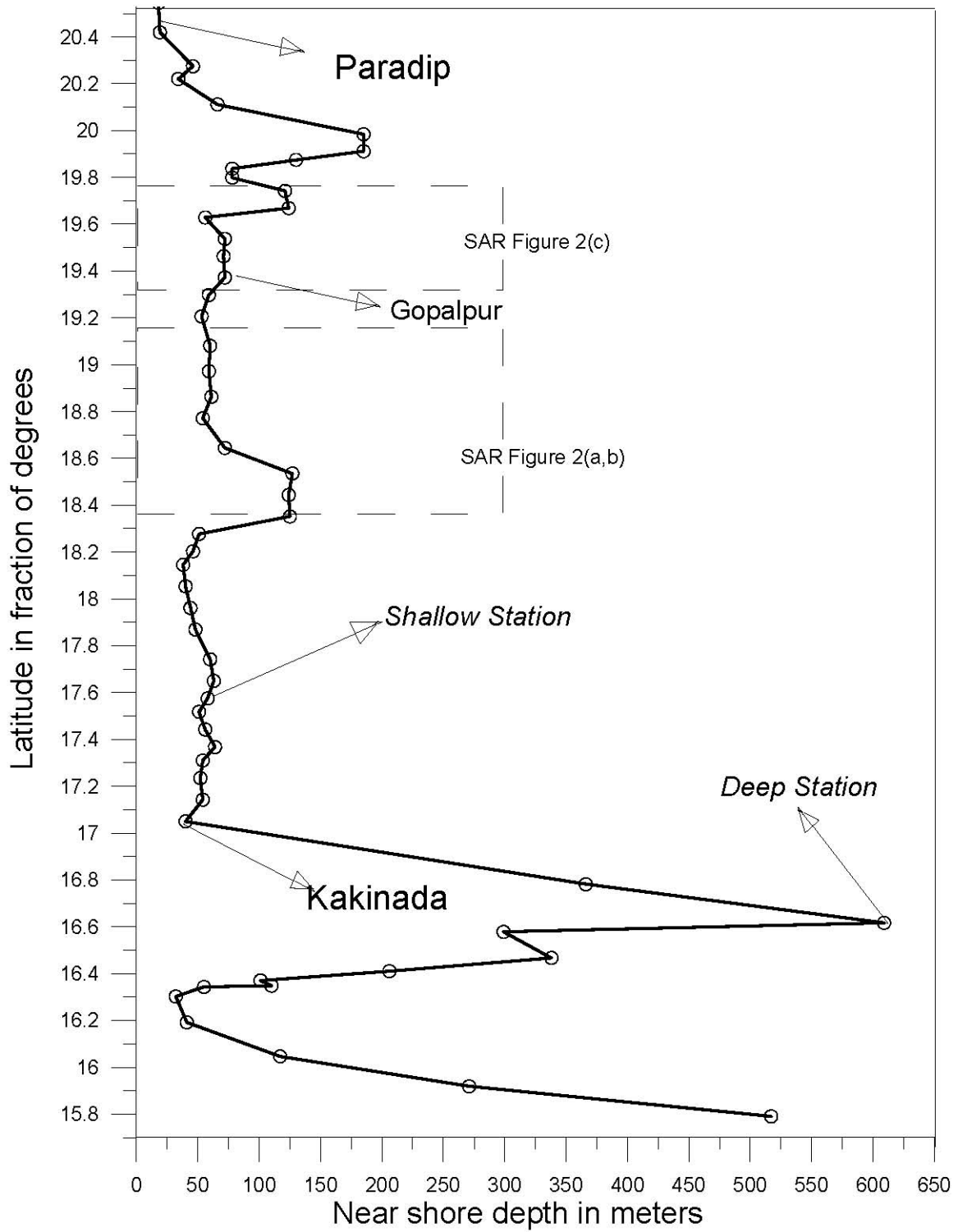
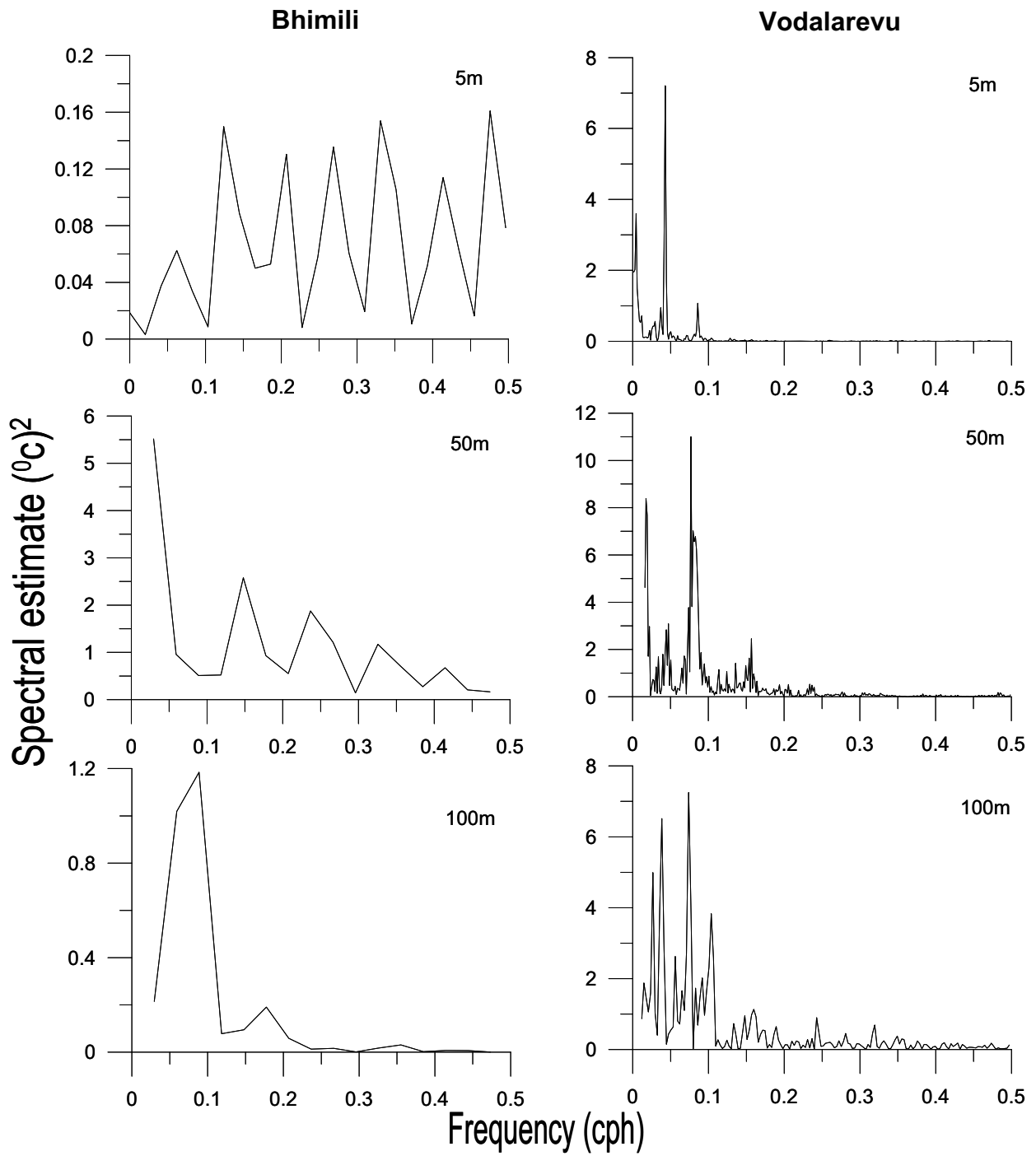


Figure 2



**Figure 3**



**Figure 4**

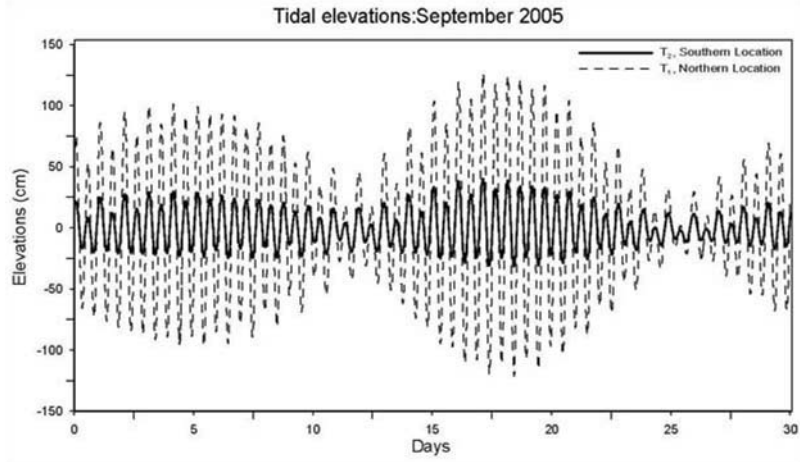


Figure 5

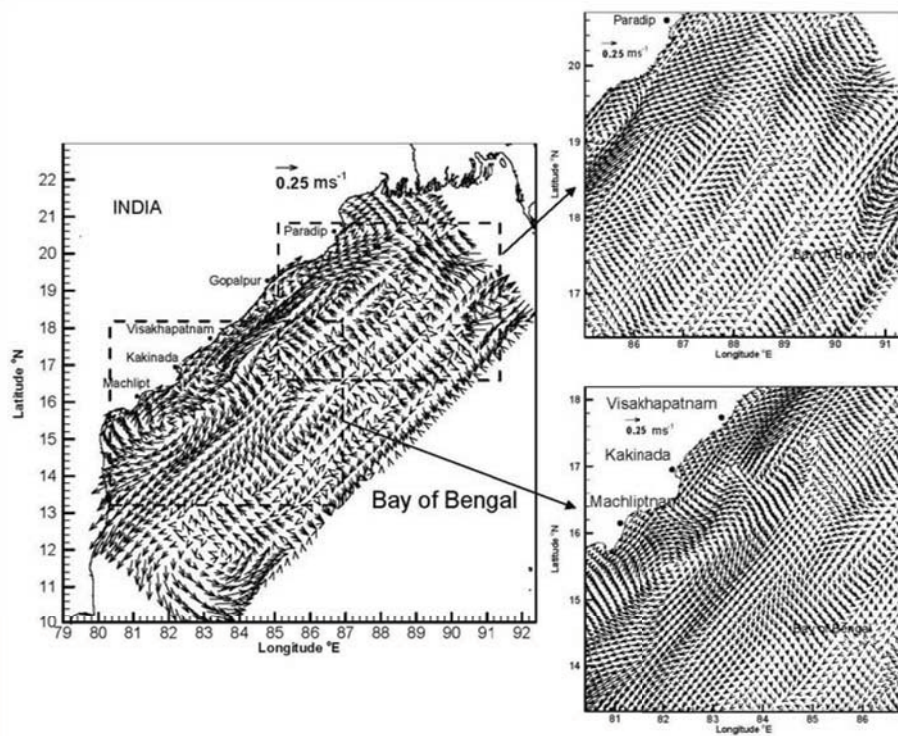
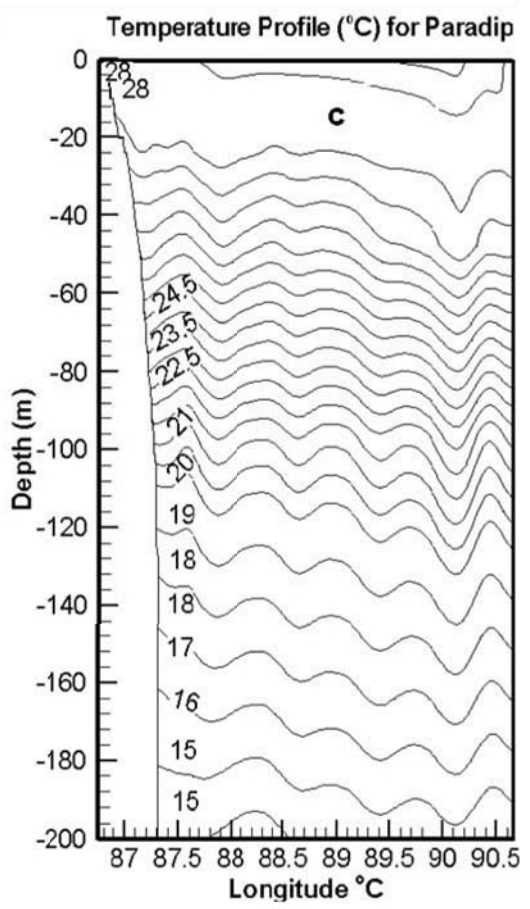
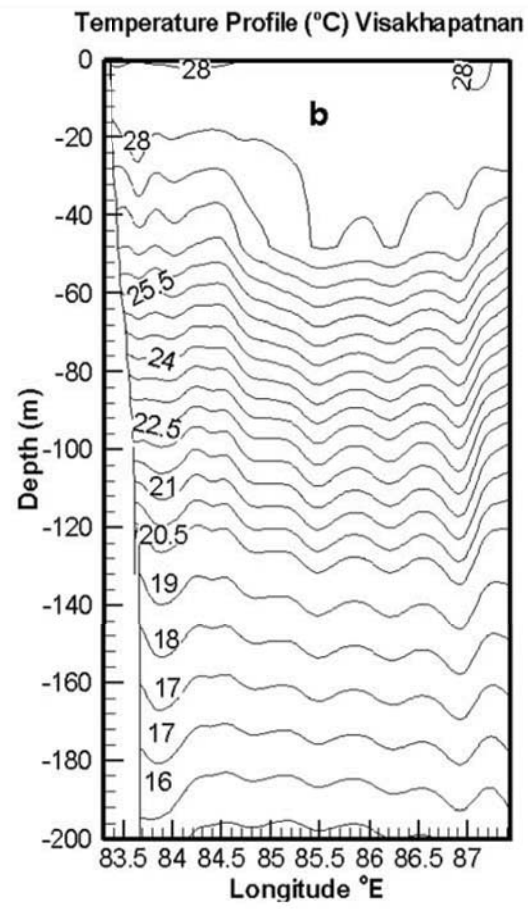
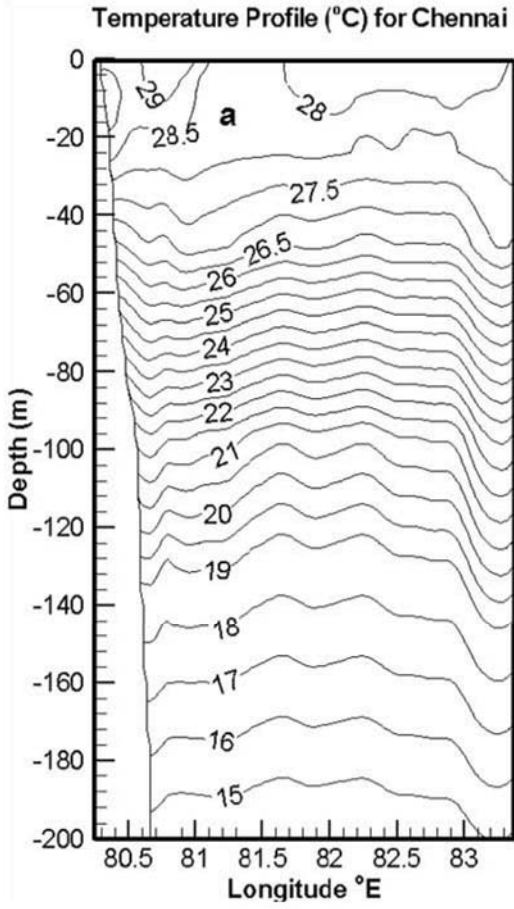
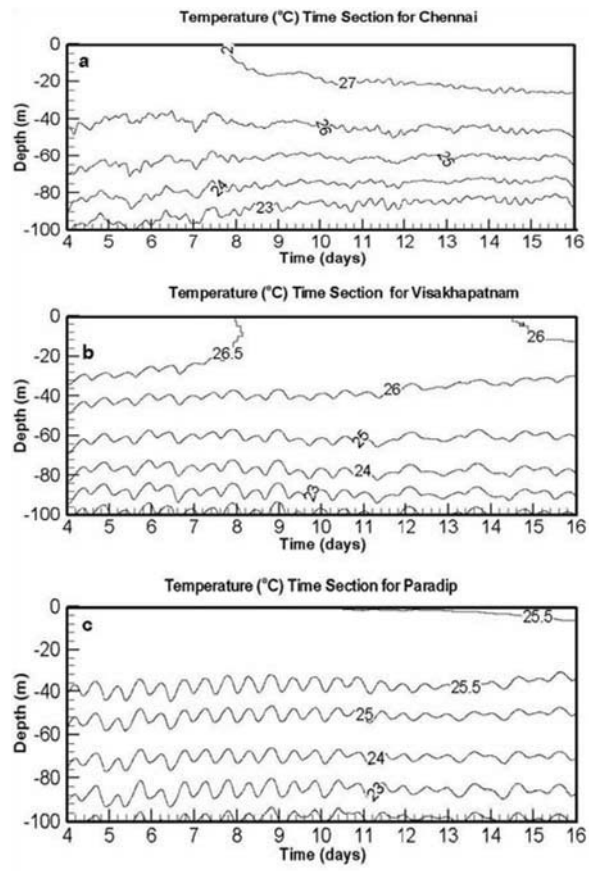


Figure 6



**Figure 7**



**Figure 8**

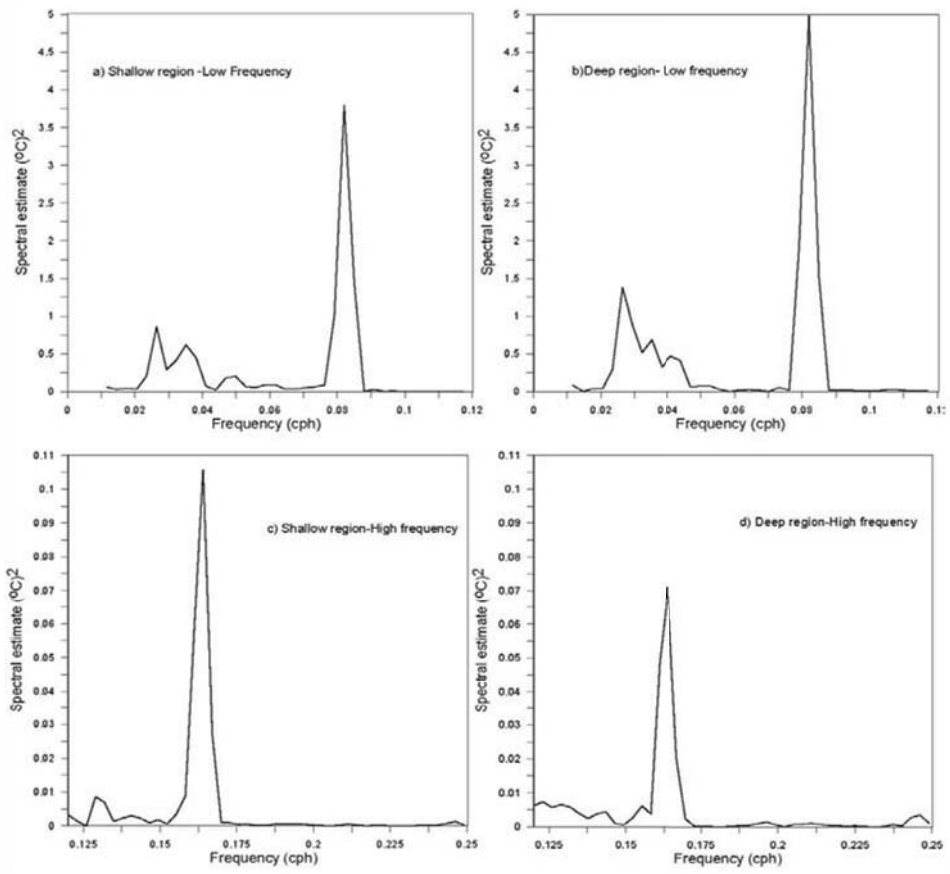


Figure 9